The Third International Conference On Structure, Processing And Properties Of Materials, SPPM2010
24-26 February 2010, Dhaka, Bangladesh, SPPM2010 C04

Microstructural and Substructural Variations during Symmetric and Asymmetric Cyclic Loading of AISI 304LN Stainless Steel

***K Dutta*[1], *S Sivaprasad*[2], *S Tarafder*[2], *K K Ray*[3]**

[1]Department of Metallurgical and Materials Engineering, National Institute of Technology, Rourkela-769008, India.

[2]Materials Science and Technology Division, National Metallurgical Laboratory, Jamshedpur-831007, India.

[3]Department of Metallurgical and Materials Engineering, Indian Institute of Technology, Kharagpur-721302, India.

Abstract

The primary aim of this investigation is to examine the influence of symmetric and asymmetric cyclic loading on (i) accumulation of plastic strain that occur during cyclic deformation of AISI 304 LN stainless steel and (ii) the attendant in-situ microstructural and substructural variations. Stress-controlled cyclic tests have been carried out at 300 K for positive and zero mean stress levels with varying stress amplitudes in order to attain both symmetric and asymmetric loading conditions. Cyclically deformed samples were studied using XRD and TEM to assess the possible structural alterations. The results highlight that the nature of strain accumulation is dependent on the combinations of mean stress and stress amplitude. Strain accumulation is more in asymmetric loading compared to that in symmetric loading. TEM and XRD results indicate that considerable amount of austenite transforms to martensite during asymmetric cyclic loading and the amount of martensite varies with the nature of the imposed stresses. It is observed that dislocation cells and tangles preferably form due to asymmetric loading. The nature of the substructure in asymmetrically loaded specimens is significantly different than that observed in specimens subjected to symmetric loading.

Keywords: Cyclic loading, Symmetric loading, Asymmetric loading, Strain accumulation.

1.0 INTRODUCTION

Structural components in critical engineering sectors may be subjected to several types of cyclic loading during their service. These may be broadly classified as symmetric (mean stress = 0) or asymmetric (mean stress ≠0) cyclic loading. Imposition of asymmetric stress cycle can lead to strain accumulation in engineering components [1]. This is one of the serious issues in critical engineering structures such as in nuclear power plants since the accumulated plastic strain governs the life of these engineering components in low cycle fatigue (LCF). It is generally noted that accumulation of this type of plastic strain decreases fatigue life [2] of engineering components, and limits the predictive capability of the Coffin-Manson relation [3]. It is therefore important to understand strain accumulation behaviour of materials in order to safe guard engineering components or structures in both symmetric and asymmetric loading conditions. The existing studies provide critical but varied views on strain accumulation behaviour under uniaxial or multiaxial loading conditions for cyclic hardening and cyclic softening type metallic materials as well as polymers and solders. In spite of this, more experimental investigations are required to refine our concepts on comparative assessment of strain accumulation under symmetric and asymmetric loading conditions. For example, most of the earlier investigations related to this type of strain accumulation addresses the mechanics of materials; but micro-mechanisms such as the possible effect of in-situ substructural and microstructural changes during cyclic tests has not been carefully dealt with in the earlier investigations.

It is well known that austenitic stainless steels are unstable upon monotonic or cyclic deformation and these readily exhibit transformations of austenite to martensite [4]. The martensitic transformation occurs when austenitic stainless steels are deformed at temperatures below M_d, a temperature below which deformation induced martensitic transformation takes place. In 304 type stainless steels formation of martensite even at room temperature is not ruled out. Since martensitic transformation

depends upon the extent of deformation, it is naturally expected to interfere with the strain accumulation during symmetric and asymmetric loading. The aim of this investigation is to examine the nature of strain accumulation in AISI 304LN stainless steel with respect to variation of sub-structure and transformation of austenite to martensite, through stress-controlled fatigue tests, at various combinations of mean stress and stress amplitude. The sub-structural and microstructural changes due to cyclic loading experiments have been examined with the help of XRD and TEM.

2.0 EXPERIMENTAL

The chemical composition of the selected AISI 304LN stainless steel is Fe–0.03C–18.55Cr–9.50Ni–0.54Si–0.028P–0.014S–0.1N–1.80Mn (all in wt.%). The steel was available in the form of a pipe of 320 mm outer diameter and 25 mm wall thickness. Sample blanks with approximate cross-sections of 12 mm x 12 mm were cut from the as received material for examining its microstructure and for determining hardness. The microstructural examinations were carried out with the help of an optical microscope (Leica, model: DMILP, USA) connected to an image analyzer (Software: Biovis Material Plus, Version: 1.50, India). The hardness measurements were done with the help of a Vickers hardness tester (Leco, model: LV 700, USA) using an indentation load of 20 kgf. Tensile tests were carried out on cylindrical specimens of 6 mm diameter and 25 mm gauge length at a nominal strain rate of $1x10^{-3}$ s^{-1} at 300 K.

Specimens with 7 mm diameter and 13 mm gauge length were prepared for stress-controlled fatigue tests. These were fabricated from the pipe in such a manner that the loading axis coincides with the pipe axis. Stress-controlled fatigue experiments were carried out at room temperature using 100 kN servo-electric testing system (Instron, model: 8862, UK). The system was attached to a computer for test control and data acquisition. All tests were done in stress-control mode till fracture using triangular waveform at a constant stress rate of 50MPa /s. The variables that have been considered for these tests are stress amplitude (σ_a), and mean stress (σ_m). Based on the employed test controls, the tests can be classified into three categories: (i) constant σ_a with varying σ_m, (ii) constant σ_m with varying σ_a and (iii) $\sigma_m = 0$. The combinations of the adopted σ_a and σ_m for each test are listed in Table 1. It may be noted that for all the tests having $\sigma_m > 0$, the specimens have been subjected to deformation under tension-compression cycles. The strain measurements during cyclic deformation were made using an axial extensometer having 12.5 mm gauge length. During each test, the stress-extension as well as the actuator displacement data were continuously recorded with an aim to acquire at least 200 data points per cycle for further analyses. Transverse sections from the gauge portion of the specimens were cut after the fatigue tests and were subjected to XRD analyses using Cu Kα radiation. These analyses were made at a scan rate of 1.5° per minute using a high resolution X-ray diffractometer (Philips, model: PW1710, UK). In addition, thin slices (~0.5 mm thick) were also cut from the gauge section of the tested samples for preparing TEM samples using a slow speed saw (Buehler, USA). The slices were then thinned sequentially by manual polishing on emery paper, dimpled and ion milled prior to TEM studies. TEM studies were carried out using a 200 keV transmission electron microscope (JEOL, model: JEM 2100, Japan).

Table 1: Selected σ_m and σ_a values for fatigue tests.

Sl. No.	σ_m (MPa)	σ_a (MPa)
1	0	420
2	50	300, 350, 400
3	100	300, 350, 400
4	150	300, 350, 400

3.0 RESULTS AND DISCUSSION

The characteristics of the microstructural features and conventional mechanical properties are described in section 3.1 while the strain accumulation behaviour of the material is discussed in section 3.2 to section 3.6.

3.1 Microstructural Characteristics and Mechanical Properties

The microstructure of the as received AISI 304LN stainless steel exhibits nearly equiaxed austenite grains with annealing twins**.** The average grain size of the steel is estimated as 65 ± 4.3 μm and its Vickers hardness (HV_{20}) is 205. The average tensile properties of the steel have been determined

from three experiments and the results can be summarized as: yield strength 340±4 MPa, tensile strength: 683±3 MPa and percentage elongation: 70.6±1.2 %.

3.2 Effect of Symmetric Cyclic Loading on the Nature of Strain Accumulation

Typical hysteresis loops generated from the fatigue tests carried out under symmetric loading (i.e. $\sigma_m = 0$) are shown in Fig. 1a and the corresponding strain accumulation behaviour with increasing number of cycles is shown in Fig. 1b. The results indicate that strain accumulation under symmetric loading is not significant. Only a maximum of 6% strain is accumulated while $\sigma_m = 0$ and $\sigma_a = 420$ MPa and it decreases for decreasing σ_a. The results are in accordance with some earlier investigations where it has been reported that no significant strain accumulation occurs under symmetric loading.

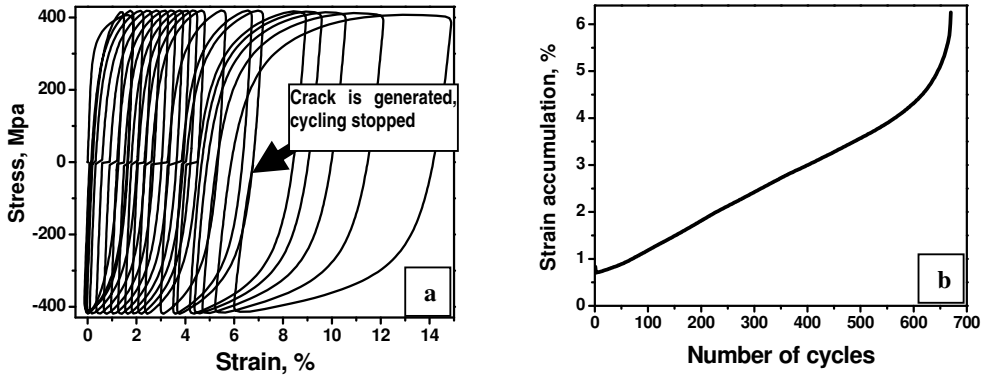

Figure 1. Typical (a) hysteresis loops generated during symmetric cyclic loading for the steel (all the cycles are not shown in the figure) and (b) variation of strain accumulation with number of cycles at a loading condition of $\sigma_m = 0$, and $\sigma_a = 420$ MPa.

The nature of strain accumulation during symmetric loading can be described using the dislocation substructure which formed during cyclic tests. The number of dislocations those generate during the forward cycle are comparable with those generated during the backward cycle but a considerable part of these gets annihilated. This phenomenon reduces strain accumulation in symmetric cyclic loading.

3.3 Effect of Asymmetric Cyclic Loading on the Nature of Strain Accumulation

The results of cyclic tests conducted under different combinations of mean stress and stress amplitude are discussed in this section.

3.3.1 Effect of stress amplitude at constant mean stress

Variations of strain accumulation (ε_p) with number of cycles (N) for varying σ_a at constant σ_m levels of 50, 100 and 150 MPa were examined and a typical illustration is shown in Fig. 2a. The results in

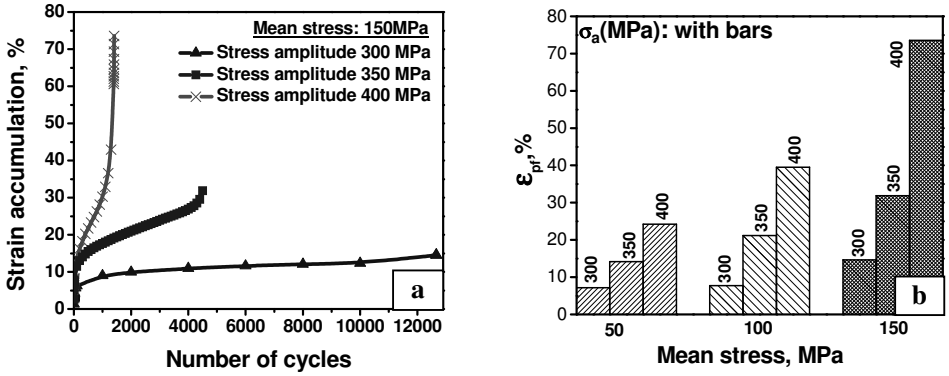

Figure 2. (a) Variation of strain accumulation with number of cycles for varying σ_a and at constant σ_m levels: $\sigma_m = 150$ MPa, (b) histograms showing variations of ε_{pf} with σ_m.

Fig. 2a indicates that ε_p monotonically increases with increasing N for any combination of σ_a and σ_m. In addition, at a constant σ_m and at any specific N value, the magnitude of ε_p increases with increasing

σ_a. The variations in total accumulated strain (ε_{pf}) at failure (i.e. N=N_f) with increasing level of σ_m at different σ_a values are summarized in Fig. 2b; the results in this figure illustrate increase in ε_{pf} with increasing level of σ_m. When σ_a is altered between 300 and 400 MPa, the magnitudes of ε_{pf} increase from 7.2 to 24.2 % at σ_m = 50 MPa, from 7.7 to 39.5 % at σ_m = 100 MPa and from 14.6 to 73.6 % at σ_m = 150 MPa. The observed nature of increase in ε_p with σ_a is in good agreement with the trend of results reported by Kang et al. [5] in SS304 stainless steel and that by Gupta et al. [6] in SA333 Gr. 6 piping steel.

The results presented in Fig. 2a infer that for a given σ_m level, fatigue life (N_f) of the material decreases with increasing ε_{pf}. The decrease in N_f with increasing σ_a for various σ_m values is compiled in Fig. 3. For example, for the combination of σ_m = 150 MPa and σ_a = 300 MPa, failure of a specimen occurs at 12661 cycles but for the combination of σ_m = 150 MPa and σ_a = 400 MPa, its fatigue life reduces to 1403 cycles (Fig. 3). Kang et al. [5] have shown that for the combination of σ_m = 65 MPa and σ_a = 325 MPa, failure occurs after 3000 cycles for solution annealed SS 304 steel; for nearly similar experimental conditions of σ_m = 50 MPa and σ_a = 300 MPa, the investigated 304LN stainless steel exhibits N_f = 6280 cycles. The difference in the observation can be attributed to the difference in the pre-history of the materials used in the two investigations.

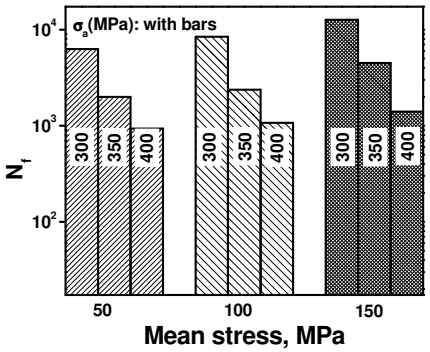

Figure 3. Histograms showing the variations of number of cycles to failure (N_f) with σ_m.

This phenomenon of strain accumulation at constant σ_m for varying σ_a can be correlated with the dislocation substructure of the material. Due to the selected nature of the loading-unloading cycles, the number of dislocations generated in the loading cycle is more than that generated in the unloading cycle; but, during load reversal, only a part of the dislocations get annihilated. As a result some amount of the generated dislocations would remain as residuals in the substructure of the investigated steel subjected to asymmetric cyclic loading. It is well known that higher is the dislocation density, higher is the accumulation of plastic strain and vice versa. Hence, it may be inferred that with increasing σ_a for a particular σ_m, total strain accumulation will increase because of the increase in the remnant dislocation density.

3.3.2 Effect of mean stress at constant stress amplitude

To understand the effect of σ_m on ε_p at constant σ_a levels, the results presented in the previous section have been re-examined as ε_p vs. N at constant σ_a. The observed behaviour is illustrated for all the investigated σ_a levels in Fig. 4**.** The increase in ε_{pf} due to increase in σ_m at constant σ_a has been discussed in the previous section. The relative increase of fatigue life with increasing σ_m can be explained in the following manner. At constant stress amplitude, if σ_m is increased, the magnitude of σ_{min} decreases, as a result, the hysteresis loop move upward. For example, at σ_a = 300 MPa when the magnitudes of σ_m are 50 and 100 MPa, that of σ_{min} are -250 and -200 MPa respectively. This phenomenon results in shifting the cyclic deformation zone more towards the tension-tension side and, as a consequence the extent of reverse plastic deformation during asymmetric cyclic loading is lower in a specimen.

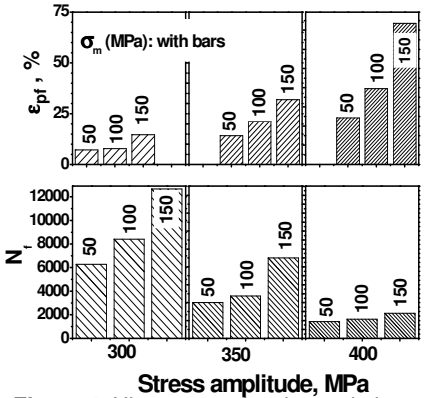

Figure 4. Histograms showing variations of total accumulated strain (ε_{pf}) and N_f with σ_a.

3.4 Saturation in Strain Accumulation

The variation in the rate of strain accumulation (RSA) with increasing number of cycles for the condition of "constant σ_a-varying σ_m" is presented in Fig. 5**.** The results indicate that $d\varepsilon_p/dN$ (or RSA) decreases with increasing number of cycles in any combination of σ_m and σ_a. Similar results were observed for "constant σ_m-varying σ_a" conditions. The decrease in RSA is rapid up to about ten cycles, after which the change in the magnitude of RSA is insignificant. The magnitude of RSA becomes almost constant after about 100 cycles for all combinations of σ_m and σ_a. In brief, it can be inferred that rapid accumulation of strain in the initial few cycles followed by attainment of a steady state in RSA

are the characteristic of the asymmetric cyclic deformation behaviour of 304LN stainless steel. The observed results infer that the change in strain accumulation is sharp in the initial cycles. This observation could possibly be attributed to the larger amount of martensitic transformation in the cycles; the martensitic transformation is known to be associated with generation of higher amount of dislocations. The attainment of steady state in RSA can be explained by the formation, movement and redistribution of dislocations associated with cyclic deformation. When the steel is subjected to cyclic deformation, new dislocations generate and results in strain hardening. These dislocations initially form tangles and subsequently lead to the formation of dislocation cells with increasing number of cycles [1]. After certain number of cycling, depending on the magnitude of the imposed cyclic strain, the newly generated dislocations assume a stable configuration and this leads to the steady state in RSA.

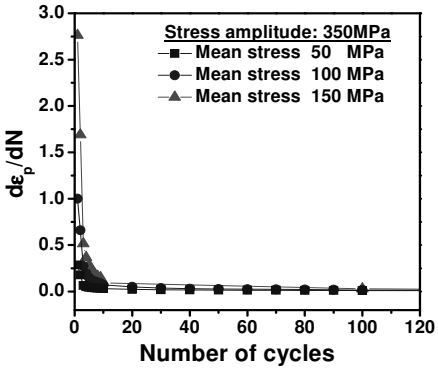

Figure 5. Variation in RSA with N (up to 100) for varying σ_m at constant σ_a.

3.5 In-Situ Variation of Substructure and Microstructure

To understand the substructural and microstructural variations associated with the deformations under-asymmetric cyclic loading of the investigated 304 LN stainless steel, the deformed specimens were examined using TEM and X-ray diffraction studies. Typical TEM bright field images obtained from thin foils cut from the transverse sections of deformed specimens are illustrated in Fig. 6. Comparison of the substructural features in Fig. 6a and 6b leads to infer that dislocation density increases with increase in the magnitude of σ_m.

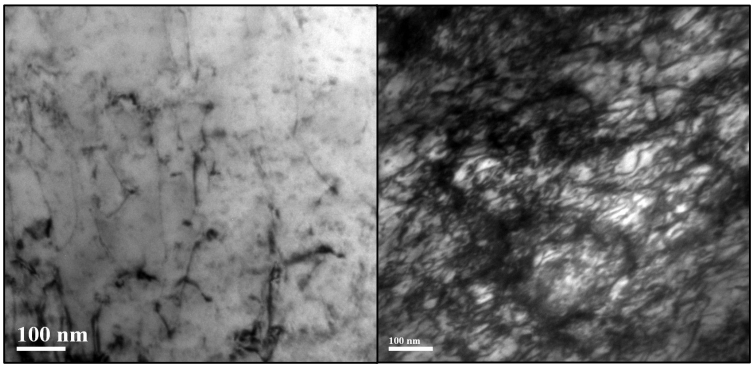

Figure 6. Typical TEM bright field images of the deformed samples with a loading condition of σ_a = 350 MPa and (a) σ_m = 50 MPa, (b) σ_m = 150 MPa.

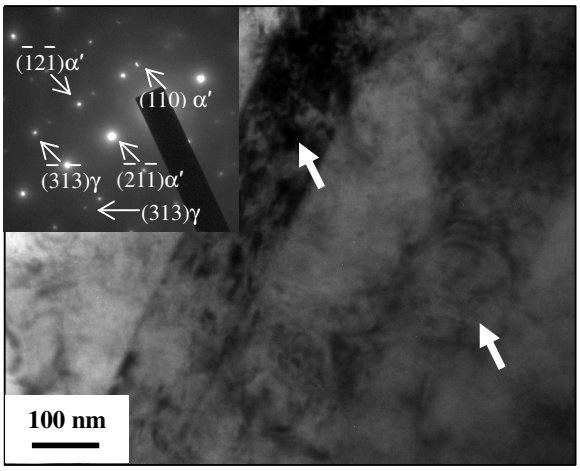

Figure 7. Formation of α'-martensite (bcc) (directed by arrow markings) with zone axis of [–113] in γ-austenite (fcc) with zone axis of [–2 3 3].

Gaudin and Feaugas [1] have reported that strain accumulation under asymmetric loading results in the formation and dissolution of dislocation cells during cycling. Dislocation cell formation is also evident from the TEM results of the present investigation.

In the as received condition, the microstructure of the investigated 304 LN stainless steel was completely austenitic. However, as a result of monotonic or cyclic deformation, this grade of stainless steel has been reported to show phase transformation from fcc austenite to metastable ε-martensite and eventually to α'-martensite [4]. TEM results unambiguously indicate that martensite forms during the asymmetric cyclic deformation. A

typical TEM bright field image along with the corresponding selected area diffraction pattern is shown in Fig. 7 to provide evidence for the formation of martensite during cyclic deformation of this steel. X-ray diffraction analyses show that both ε- martensite (hcp) and α′-martensite (bcc) peaks are present in the diffraction pattern (Fig. 8).

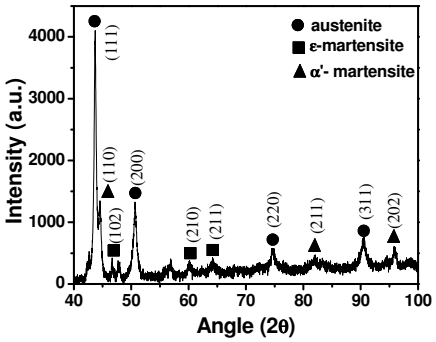

Figure 8. XRD pattern showing formation of ε-martensite and α′-martensite.

In generalization, three synergistic phenomena are taking place during asymmetric cyclic deformation of AISI 304 LN stainless steel: (i) variation in dislocation density, (ii) formation, followed by dissolution or growth or shrinkage of the dislocation cells, and (iii) martensitic transformation. It is noted that the deformation induced martensite can be stable α′ or the metastable ε□ and their role in altering the remnant dislocation density or the cyclic deformation process in influencing ε_p or N_f remains unclear at this stage. However, it can be unambiguously concluded that σ_m has more significant effect than σ_a in controlling strain accumulation behaviour of the investigated 304 LN stainless steel.

4.0 CONCLUSIONS

The results and their pertinent analyses related to the present stress-controlled cyclic loading experiments on AISI 304 LN stainless steel at room temperature lead to infer:

(1) Higher the magnitude of σ_a at constant σ_m level, higher is the ε_p, in the selected steel. Similar increase in ε_p is noted when σ_m is increased at constant σ_a. But interestingly, N_f decreases with increased ε_{pf} when σ_m is kept constant and it increases with increased ε_{pf} when σ_a is kept constant.

(2) The increase in the magnitude of ε_p at constant σ_m or at constant σ_a can be explained by the increase in remnant dislocation density. At constant σ_m, when σ_a increases the reverse plastic deformation component also increases causing additional hardening of the material and consequently N_f decreases. But for constant σ_a, cyclic plastic deformation zone of the material shifts towards tension-tension side, and this is considered to contribute a longer life.

(3) The magnitude of strain accumulation is observed to get saturated at $\geq$ 100 cycles of loading for the as-received AISI 304 LN stainless steel. The influence of the magnitude of σ_m is more predominant than that of σ_a in controlling strain accumulation of the investigated 304 LN stainless steel.

(4) TEM studies lead to infer that dislocation density of the cyclically deformed samples increases with increasing σ_m at constant σ_a. X-ray diffraction studies indicate that deformation induced martensite forms during asymmetric cyclic loading. This type of martensitic transformation also adds up new dislocations in the deformed samples.

5.0 REFERENCES

[1] Gaudin, C. and Feaugas, X., 2004. “Cyclic Creep Process in AISI 316L Stainless Steel in Terms of Dislocation Patterns and Internal Stresses,” Acta Materialia, 52, 3097–3110.

[2] Ozgen, U.C., 2007. “Kinematic Hardening Rules for Modeling Uniaxial and Multiaxial Ratcheting,” Materials and Design, 29, 1575-1781.

[3] Xia, Z., Kujawski, D. and Ellyin, F., 1996. “Effect of Mean Stress and Ratcheting Strain on Fatigue Life of Steel,” International Journal of Fatigue, 18, 335-341.

[4] De, A.K., Murdock, D.C., Mataya, M.C, Speer, J.G. and Matlock, D.K., 2004. “Quantitative Measurement of Deformation-Induced Martensite in 304 Stainless Steel by X-Ray Diffraction,” Scripta Materialia, 50, 1445-1449.

[5] Kang, G.Z., Li, Y.G., Zhang, J., Sun, Y.F. and Gao, Q., 2005. “Uniaxial Ratcheting and Failure Behaviors of Two Steels,” Theoretical and Applied Fracture Mechanics, 43, 199-209.

[6] Gupta, C., Chakravartty, J.K., Reddy, G.R. and Banerjee, S., 2005. “Uniaxial Cyclic Deformation Behaviour of SA 333 Gr 6 Piping Steel at Room Temperature,” International Journal of Pressure Vessels and Piping, 82, 459-469.